OPTIMIZATION OF A TERAWATT FREE ELECTRON LASER*

X. Huang, J. Wu†, T.O. Raubenheimer, Y. Jiao‡, S. Spampinati§, SLAC, Menlo Park, CA 94025, USA
A. Mandlekar, Monta Vista High School, Cupertino, CA 95014, USA
G. Yu, Henry M. Gunn Senior High School, Palo Alto, CA 94306, USA
P. Chu, FRIB, East Lansing, MI 48823, USA
J. Qiang, LBNL, Berkeley, CA 94720, USA

Abstract

There is great interest in generating a terawatt (TW) hard X-ray free electron laser (FEL) that will enable coherent diffraction imaging of complex molecules like proteins and probe fundamental high-field physics. A feasibility study of producing such pulses was carried out employing a configuration beginning with an SASE amplifier, followed by a "self-seeding" crystal monochromator, and finishing with a long tapered undulator. The undulator tapering profile, the phase advance in the undulator break sections, the quadrupole focusing strength, etc. are parameters to be optimized. A genetic algorithm (GA) is adopted for this multi-dimensional optimization. Concrete examples are given for LCLS/LCLS-II systems.

Introduction

Single molecule imaging and in general to study structures on the nanometer or even finer level requires more than 1.0E+13 photon/second in a pulse within femtosecond duration [1, 2, 3]. This calls for a high power FEL on the order of terawatts (TW). A promising approach to reach TW powers is to increase the energy transfer from the electrons to radiation by adjusting the undulator magnetic field to compensate for the electron energy losses, a "tapered" undulator [4]. However, to reach such high power TW FELs, previous study has shown that simply tapering the undulator for a FEL working in a Self-Amplified Spontaneous Emission (SASE) mode is not sufficient [5]. A seeded FEL is more efficient responding to the tapered undulator and can potentially bring the FEL to TW level. A proof-of-concept design based on self-seeding scheme has been developed for European XFEL [6] as well as for LCLS/LCLS-II [7] with LCLS-type electron bunch [8] and LCLS-II-type variable gap undulator.

As is well known and experimentally verified, for an undulator with constant strength, high gain, single pass FEL amplifiers reach saturation at a power level of $P_{\rm sat.} \sim \rho P_{\rm beam}$ where $P_{\rm beam}$ is the electron beam power and ρ is the FEL efficiency parameter [9]. This behavior is true for both SASE and externally-seeded configurations and arises from the growth of instantaneous energy spread and the rotation of the microbunched electrons in the ponderomotive well formed by the FEL radiation and the undulator magnetic field. For electron beam parameters corresponding to the proposed LCLS-II project at SLAC, $\rho \sim 5 \times 10^{-4}$, the nominal saturation power is $\sim$ 30 GW, far below the TW level. However, near and at saturation the microbunching fraction is large (bunching factor: $b_1 \sim 0.5$) suggesting that with proper tapering of the normalized undulator strength K, one can both trap and then decelerate a comparable fraction of the electrons to extract much greater additional power [4]. For example, currently LCLS doubles its output power to $\sim$ 70 GW using its available tapering range of $\Delta K/K \sim 0.8\%$.

The proposed LCLS-II undulators have fully tunable gaps and thus in principle can taper K fully to zero. Moreover, there is currently great interest in giving LCLS-II a self-seeding option employing the crystal monochromator scheme [10]. Consequently, a TW-level FEL starts with a SASE undulator sufficiently long to generate GW-level radiation. This radiation then passes through a crystal monochromator that results in a MW-level, nearly monochromatic wake. Following the chicane, the radiation and electron beam enter a second undulator in which first the radiation grows exponentially to saturation and then, via a tapering of K to maintain a high electron microbunching fraction, continues to strongly grow to TW power levels [7]. Similar study on TW FEL for the European X-ray FEL has been conducted [6].

We have developed an approach [11] to empirically optimize $K(z)$ tapers that maximize the output power at a fixed total undulator length. In Refs. [7, 11], we proposed to formulate the taper as a mathematical function

$$K(z) = K_0\{1 - a[(z - z_0)/(L_w - z_0)]^b\}, \qquad (1)$$

with b not necessarily an integer.

We have also considered a z-dependent optimization of the electron beam transverse size for better coupling to the radiation mode size. As described in Ref. [11], we introduce a three-segment r_b variation by linearly changing the quadrupole field strength $K_q(z)$ with z,

$$K_q(z) = \begin{cases} K_{q0}, & 0 \le z \le z_1 \\ K_q(z_1)\,[1 - f(z - z_1)], & \text{for } z_1 < z \le z_2 \\ K_q(z_2)\,[1 - g(z - z_2)], & z_2 < z \le L_w \end{cases}, \qquad (2)$$

where z_1 indicates the first K_q-variation start point, which is usually around the end of exponential growth regime; z_2 indicates the second K_q-variation start point; f can be either positive or negative, while g is usually negative.

* Work supported by U.S. Department of Energy, Office of Basic Energy Sciences, under Contract DE-AC02-76SF00515.
† Correspondence should be sent to: jhwu@SLAC.Stanford.EDU
‡ Also at Institute of High Energy Physics, Chinese Academy of Sciences, Beijing 100049, China
§ Also at University of Nova Gorica, Slovenia

The optimization is in 8-dimensional parameter space, namely, a, b, z_0, K_{q0}, z_1, z_2, f, and g with final radiation power as the objective function. A grid-scan type of optimization approach was adopted in Ref. [11]. To minimize computational expense, optimization was carried out with the GENESIS code [12] in time-steady mode, followed by fine tuning with full time-dependent runs to get better performance. For the examples studied in Ref. [7, 11], TW FEL is possible with LCLS-type electron bunch, and LCLS-II-type variable gap undulator.

Multi-Objective Genetic Algorithms – MOGA

To further improve the optimization and explore the parameter space, we adopt a Multi-Objective Genetic Algorithm. Preliminary results are reported here.

The goal of multi-objective optimization is to find the Pareto optimal front, or the set of solutions that are not inferior to any other solution in the parameter space. Traditional approaches study weighted sums of the objectives, while an evolutionary algorithm converges to the Pareto front in one run. The evolutionary algorithms (or genetic algorithms) manipulate a set of solutions (a population) toward the optimal front with operations that simulate biological evolution. Typical operators include selection that apply the evolution pressure toward the optimal front; crossover that creates new solutions (children) by combining existing solutions (parents); and mutation that alters existing solutions to create new ones. The genetic algorithms are capable of obtaining the global optimum despite the complexity of the problem. They can optimize multiple objectives simultaneously. It is easy to apply constraints in these constraints. However, it can be much slower than the gradient-based methods.

In this paper, we use the non-dominated sorting genetic algorithm NSGA-II [13] to attack the TW FEL optimization problem. The *Matlab* [14] implementation of the algorithm is modified for parallel computing via submitting multiple jobs to a cluster computer. It uses file input/output for communication between the external simulation code (GENESIS) and the control-processing environment (*Matlab*). For the time-independent simulation cases, where the individual evaluation time is short, the speed of the algorithm is limited by file I/O time. For example, the average evaluation time is 4.5 seconds on up to 60 processors, while an individual evaluation takes 20 seconds. However, we expect a much larger speed gain for the time-dependent cases. Modifications are also made to the algorithm to control the convergence behavior during the run.

LCLS-II Taper Optimization

In Ref. [11], we did the 8-dimensional grid-scan optimization as mention above. The objective function is the total FEL radiation power $P_{\rm FEL}$. Here we introduce a second parameter, the radiation pseudo-emittance, $\varepsilon_\gamma \equiv \sigma_r\sigma_\theta$, where σ_r is the transverse radiation size, and σ_θ is the rms diffraction angle of the radiation at the undulator end. The focusing scheme is the same as in Eq. (2). We first further explore the taper model by adding higher-order terms.

Cubic 9 variables In this case, we model the taper as

$$K(z)=K_0[1-a_1(\frac{z-z_0}{L_w})-a_2(\frac{z-z_0}{L_w})^2-a_3(\frac{z-z_0}{L_w})^3], \quad (3)$$

where a_i for $i = 1$, 2, and 3 are the parameters to characterize the taper strength. Hence, we have a total of 9 optimization parameters: 4 from the taper model as in Eq. (3) and 5 from the focusing model as in Eq. (2).

Quartic 8 variables Here, we model the taper as

$$K(z)=K_0[1-b_2(z-z_0)^2/{L_w}^2-b_4(z-z_0)^4/{L_w}^4], \quad (4)$$

where b_i for $i = 2$ and 4 modle the taper strength. Hence, we have a total of 8 parameters: 3 from the taper model as in Eq. (4) and 5 from the focusing model as in Eq. (2).

Phase shifter In Refs. [7, 11], we guarantee that in the undulator breaks, the phase advance of the light with respect to the electron beam is the minimum integer number N_b of 2π. Here, we allow the phase advance to deviate from an integer number of 2π, and include this deviation as optimization parameters. Based on the study in Ref. [11], the most effective ones should be the first a few phase shifters after the exponential growth stops.

NSGA-II setup As mentioned above, we have 2 objective functions: $P_{\rm FEL}$ and the pseudo-emittance ε_γ. Depending on the taper model, we will have 8 or 9 variables without phase shifters. We also study cases including 7 phase shifters. We set 600 for the population size and the termination condition is to run either about 100 generations or if the results have converged. We adopt evolving mutation and crossover probability.

Results

Let us now present some concrete results. The FEL resonant wavelength is $\lambda_r = 1.5$ Å, the undulator rms strength before tapering is $a_w = 2.47$ with period of $\lambda_w = 3$ cm and total length of $L_w \approx 113$ meter. The undulator is composed of sections with magnetic length of $L_m = 3.4$ m and break length of $L_b = 60$ cm. The electron bunch centroid energy is $E_0 = 13.635$ GeV with a slice energy rms spread of $\sigma_E = 1.3$ MeV, and is compressed to have peak current of $I_{pk} = 4$ kA. The slice normalized emittance is $\varepsilon_n = 0.3$ μm-rad in both x- and y-plane.

Quadratic 8 variable without phase shifter To set up the simulation, we give each of the 8 parameters a range as in Table 1. The solutions with the highest power are shown as the 4^{th}-column in Table 1. The generation-by-generation evolution of the optimization is shown in Fig. 1, where the results converge at around 100 generations.

ISBN 978-3-95450-115-1

Table 1: Quadratic 8 variables with and without phases

Parameter	Low	Up	without	with
a	0.01	0.3	0.1043	0.114
z_0 (m)	10	40	13.1	16.8
b	1.1	3.3	2.0359	2.072
K_{q0} (T/m)	20	40	34.4	34.9
f	-0.005	0.005	0.0018	0.0008
z_1 (m)	20	80	80.0	74.3
g	-0.01	0.01	0.0061	0.0022
z_2 - z_1 (m)	0	70	28.9	9.3

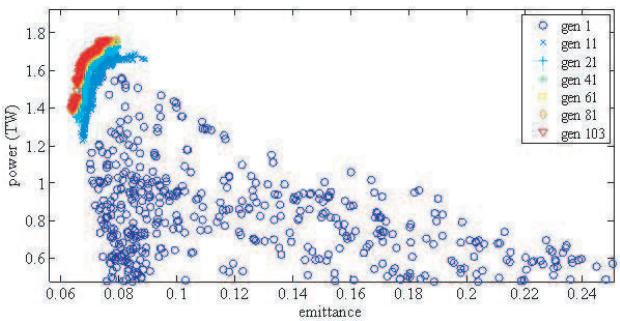

Figure 1: The generation-by-generation evolution of the optimization for the quadratic 8 variable case.

Quadratic 8 variable with 7 phase shifters The solutions are shown as the 5^{th}-column in Table 1. We treat the phase advance in the break after undulator section 5 to 11 as variables. So, we have 15 parameters for optimization.

Table 2: Different taper model with or without phase shifter

Case	$P_{\rm FEL}$ (TW)	ε_γ (μm-rad)	Taper Ratio	Capture Ratio %
1	1.760	0.0753	0.075	43.0
2	1.830	0.0790	0.0816	41.1
3	1.805	0.0751	0.0762	43.4
4	1.743	0.0702	0.0722	44.3
5	1.842	0.0794	0.0804	42.0
6	1.799	0.0757	0.0783	42.1

Summary Similarly, we did some other combination of different taper model: the cubic 9 variables, and the quartic 8 variables with or without the 7 phase shifters. The results are summarized in Table 2.

The focusing scheme is the same in all cases, *i.e.* as what is described in Eq. 2. Differences are for different taper model and with or without phase shifter optimization. To clarify, the different cases are as the follows:

- Case 1, quadratic taper model as in Eq. (1) without phase shifter optimization, so a total of 8 variables.

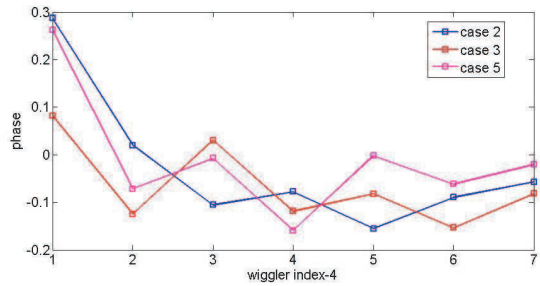

Figure 2: The phase shifter optimized phase value.

- Case 2, quadratic taper model as in Eq. (1) with 7 phase shifter optimization, so a total of 15 variables.
- Case 3, quadratic 8 variable as in Case 1, running to generation 47 with a FEL power of $P_{\rm FEL} = 1.753$ TW. With this set of 8 variables fixed, we optimize the 7 undulator break phase shifters. This is different from Case 2, because in the Quadratic 8 variable with 7 phase shifters, we optimize the 15 variables from the very beginning simultaneously.
- Case 4, cubic taper model as in Eq. (3) without phase shifter optimization, so total of 9 variables.
- Case 5, cubic taper model as in Eq. (3) with 7 phase shifter optimization, so total of 16 variables.
- Case 6, quartic taper model as in Eq. (4) without phase shifter optimization, so total of 8 variables.

As in Table 2, it seems that the higher-order terms, *i.e.* the cubic term and the quartic term in Eqs. (3) and (4) can help to improve the energy extraction efficiency from the electron beam to the photon beam. The phase shifter optimization can increase the final radiation power as well. The optimized phase values for different cases are shown in Fig. 2. The physics and the optimization should be further explored. To understand more about the optimization, we also list the effective capture ratio in Table 2.

REFERENCES

[1] H. N. Chapman *et al.*, Nature **470**, 73 (2011).
[2] M. M. Seibert *et al.*, Nature **470**, 78 (2011).
[3] A. Fratalocchi *et al.*, Phys. Rev. Lett. **106**, 105504 (2011).
[4] N.M. Kroll *et al.*, IEEE J. Quantum Electronics, **QE-17**, 1436 (1981).
[5] W.M. Fawley *et al.*, NIM **A 483**, 537 (2002).
[6] G. Geloni *et al.*, DESY 10-108 (2010).
[7] W. M. Fawley *et al.*, in Proc. FEL Conference, 2011, TUOA4.
[8] P. Emma *et al.*, Nature Photonics **4**, 641 (2010).
[9] R. Bonifacio *et al.*, Opt. Commun., **50**, 373 (1984).
[10] G. Geloni *et al.*, J. Modern Optics **58**, 1391 (2011)
[11] Y. Jiao *et al.*, PRSTAB **15**, 050704 (2012).
[12] S. Reiche, Nucl. Instrum. Methods **A 429**, 243 (1999).
[13] K. Deb *et al.*, IEEE Transactions On Evolutionary Computation **6**, 182 (2002).
[14] http://www.mathworks.com/.